

Tissint is a Rosetta stone deciphering Noachian magmatic activities and dynamic events in Mars young history

Tissint is a Rosetta stone deciphering Noachian magmatic activities and dynamic events in Mars young history

El Goresy Ahmed^{1*}, Philippe Gillet², 宮原 正明³, 大谷 栄治³, 小澤 信⁴, Yangting Lin⁵, Lu Feng⁵, S. Escherig²
Ahmed El Goresy^{1*}, Philippe Gillet², Masaaki Miyahara³, Eiji Ohtani³, Shin Ozawa⁴, Yangting Lin⁵, Lu Feng⁵, S. Escherig²

¹Bayerisches Geoinstitut, Universitat Bayreuth, ²Ecole Polytechnique Federale de Lausanne, ³Graduate School of Science, Tohoku University, ⁴National Institute of Polar Research, ⁵Institute of Geology and Geophysics, Chinese Academy of Sciences
¹Bayerisches Geoinstitut, Universitat Bayreuth, ²Ecole Polytechnique Federale de Lausanne, ³Graduate School of Science, Tohoku University, ⁴National Institute of Polar Research, ⁵Institute of Geology and Geophysics, Chinese Academy of Sciences

Tissint is a new witnessed Martian meteorite. NWA 6162 is a new Martian meteorite find. Both are Al-poor ferroan basalts and classified as shocked phyric and depleted shergottites. An array of numerous thin shock-melt veins and few thick shock-melt veins pervasively intersect Tissint each containing high-pressure assemblage. Shock features in Tissint could tentatively be assigned to three dynamic episodes on Mars with distinct textural settings, abundance and compositions of the high-pressure inventories;

The first dynamic event induced total melting of feldspar and its quenching at high-pressure to maskelynite glass along with liquidus jadeite, latter confirmed by the characteristic Raman analysis. Pervasive melting of pyroxene, pyrrhotite and titanomagnetite also took place at this episode as deduced from the spatial relationships. Acicular jadeite crystals grew on the pyroxene surface into the maskelynite liquid at high-pressure. Textural and spatial relationship of the maskelynite pools and the bordering jadeite suggests that jadeite was quenched from the plagioclase melt at P: 10~19 GPa and T: 2000 degree. This dynamic event entirely destroyed the original igneous texture and reset the radiometric age at the impact-melting episode.

An array of thin shock-melt veins fan through the whole Tissint. They penetrate Tissint along pyroxene grain boundaries and cut through the jadeite bands. An assemblage of idiomorphic liquidus high-pressure majorite-pyropess and magnesiowustite fill these shock melt veins.

Another type of shock-melt veins that cross cuts pyroxene contains considerably crushed, fragmented and mobilized majorite-pyropess + magnesiowustite grains. Fragmentation and mobilization could have probably taken place in a later dynamic or more likely a Martian tectonic event subsequent to the first vein formation episode.

Fayalite-rich rims of the originally zoned olivine partly inverted to polycrystalline ringwoodite either in coarse ringwoodite domains in the originally fayalite-rich rims or in polycrystalline aggregate in the original olivine suggesting formation by incoherent olivine-ringwoodite phase transition. The Raman spectrum also shows several original olivine crystals adjacent to shock-melt veins were shock dissociated to a fine-grained assemblage of MgSiO₃ perovskite + magnesiowustite. Some olivine grains entrained in the thick shock-melt veins of NWA 6162 depict dissociation textures to MgSiO₃ perovskite + magnesiowustite. This strongly suggests that the olivine dissociation took place at equilibrium peak-shock pressure slightly overstepping 25 GPa and at T above 700 degree. The three deciphered dynamic events on Tissint, and NWA 6162 lithologies entirely erased their igneous integrities.

Tissint and NWA 6162 share many of the encountered pervasive shock-melting effects and high-pressure phase transformations with other phyric and basaltic shergottites, unfortunately not recognized by numerous Mars scholars advocating for several volcanic eruptions younger than 575 Ma that is discrepant with the dynamic induced effects documented by us. We cast considerable doubt on the radiometric ages shorter than 575 Ma reported in the past 39 years to be the igneous crystallization ages, especially when considering their coincidence with a well-established late dynamic event. These short ages resulted from partial or total shock-induced age resetting.

ラマンおよびカソードルミネッセンス分光分析を用いたシリカ高压相の同定 Identification of high-pressure silica polymorphs using Raman and cathodoluminescence spectroscopy

鹿山 雅裕^{1*}, 大谷 栄治², 宮原 正明², 金子 詳平², 西戸 裕嗣³, 関根 利守¹, 小澤 信⁴, 蜷川 清隆⁵, 平尾 直久⁶
Masahiro KAYAMA^{1*}, OHTANI, Eiji², MIYAHARA, Masaaki², KANEKO, Shohei², NISHIDO, Hirotsugu³, SEKINE, Toshimori¹, OZAWA, Shin⁴, NINAGAWA, Kiyotaka⁵, HIRAO, Naohisa⁶

¹ 広島大学大学院理学研究科地球惑星システム学専攻, ² 東北大学大学院理学研究科地学専攻, ³ 岡山理科大学生物地球学部生物地球学科, ⁴ 国立極地研究所, ⁵ 岡山理科大学理学部応用物理学科, ⁶ (財)高輝度光科学研究センター

¹Department of Earth and Planetary Systems Science, Graduate School of Science, Hiroshima University, ²Department of Earth and Planetary Materials Science, Graduate School of Science, Tohoku University, ³Department of Biosphere-Geosphere Science, Okayama University of Science, ⁴National Institute of Polar Research, ⁵Department of Applied Physics, Okayama University of Science, ⁶Japan Synchrotron Radiation Research Institute, 1-1-1 Kouto Sayo, Hyogo 679-5198, Japan.

High-pressure silica polymorphs such as seifertite and stishovite are known in Martian and lunar meteorites and the existence and stability provide constraint on condition of shock pressure and post-temperature in impact event that the parent body have experienced. Transmission electron microscopy and Raman spectroscopy have been attempted to identify post-stishovite, whereas it was not successful to determine the structure due to potential vitrification or transition into other phase by the irradiation. Although cathodoluminescence (CL) spectroscopy has been also conducted, no characteristic signal was obtained from post-stishovite. Only XRD analysis allows us to identify the structure, where silica minerals are excavated with a focused ion beam (FIB) system from meteorite. Therefore, it is necessary for identification of micron-order high-pressure silica polymorphs in precious extraterrestrial materials to develop a new method without sample preparation. In this study, Raman and CL spectroscopy has been performed for synthetic and meteoritic silica minerals, the results of which can identify the polymorphs with high-spatial resolution as nondestructive analysis.

The block pieces of silica grains in Zagami, NWA2975 and NWA4734 meteorites, excavated with FIB system, were identified as seifertite, stishovite and cristobalite by a synchrotron X-ray at Spring-8 BL-10 and were employed for Raman and CL spectroscopy. Synthetic seifertite and stishovite were also analyzed as reference materials to compare their CL and Raman data with meteoritic silica polymorphs.

Reflected-light microscopy and backscattered electron image of synthetic seifertite show numerous polycrystalline grains (<50 micrometers in diameter) with two orthogonal sets of bright and dark lamellae. Wedge-shaped silica grains in the meteorites also display the tweedlike internal microstructure and are surrounded by radiating cracks extended from the surface to the neighbor maskelynite or clinopyroxene.

Raman spectra of synthetic seifertite consist of pronounced peaks at 380, 515, 564, 739 and 796 cm^{-1} and weak peaks at 401, 496, 539, 547, 606 and 749 cm^{-1} , of which the Raman shifts and relative intensities are corresponding to those calculated within the density-functional perturbation theory for seifertite. Similar Raman peaks are also obtained from silica grains in the meteorites, implying characteristic signals of seifertite. Synthetic and meteoritic seifertite has the distinct Raman peaks after the prolonged laser beam, X-ray and electron irradiation. Although seifertite was considered to be highly unstable phase and therefore the post-shock temperature of meteorite containing seifertite was supposed to be relatively low, it might survive post-shock thermal history with a higher temperature than the expected.

CL spectra of synthetic and meteoritic seifertite show emission bands at 330 and 380 nm in the UV region, which can be deconvoluted into emission components centered at 3.79 and 3.25 eV. The peak wavelengths are distinct from those obtained from other silica polymorphs such as stishovite (3.15 and 3.04 eV) and cristobalite (3.02 and 2.63 eV). CL images of synthetic seifertite exhibit polycrystalline grains with bright rim and vein-shaped luminescent interior on dull background, which may be caused by formation and elimination of lattice defect due to high pressure and dynamic recrystallization. The components, therefore, may be assigned to pressure-induced defect center. The emission intensities of the components centered at 3.79 and 3.25 eV appear to depend on the inferred shock pressure on the meteorites reported by previous studies and should be closely related to the defect density. Therefore, CL and Raman spectroscopy enables identification of silica polymorphs with high-spatial resolution and without destruction, and provides valuable information on impact history concerning shock pressure and post-temperature.

キーワード: ラマン分光分析, カソードルミネッセンス, シリカ高压相, ザイフェルタイト, スティショバイト, 隕石
Keywords: Raman spectroscopy, Cathodoluminescence, High-pressure silica polymorphs, Seifertite, Stishovite, Meteorite

IN SITU ISOTOPE ANALYSES OF ORGANIC CARBON FROM THE TISSINT MARTIAN METEORITE: EVIDENCE FOR A BIOGENETIC ORIGIN

Lin YT^{1*}, A. El Goresy², S. Hu¹, J. Zhang¹, P. Gillet³, Y. Xu¹, J. Hao¹, M. Miyahara⁴, Z. Ouyang⁵, E. Ohtani⁴, L. Xu⁶, W. Yang¹, L. Feng¹, X. Zhao¹, J. Yang⁷, S. Ozawa⁸
YT Lin^{1*}, A. El Goresy², S. Hu¹, J. Zhang¹, P. Gillet³, Y. Xu¹, J. Hao¹, M. Miyahara⁴, Z. Ouyang⁵, E. Ohtani⁴, L. Xu⁶, W. Yang¹, L. Feng¹, X. Zhao¹, J. Yang⁷, S. Ozawa⁸

¹Institute of Geology and Geophysics, Chinese Academy of, ²Bayerisches Geoinstitut, Universitat Bayreuth, 95447 Bayreuth, Germany, ³EPFL, CH-1015, Lausanne, Switzerland, ⁴Tohoku University, Sendai 980-8578, Japan, ⁵Institute of Geochemistry, CAS, Guiyang, China, ⁶National Astronomical Observatories, CAS, Beijing, China, ⁷Guangzhou Institute of Geochemistry, CAS, Guangzhou, China, ⁸National Institute of Polar Research, Tokyo, Japan

¹Institute of Geology and Geophysics, Chinese Academy of, ²Bayerisches Geoinstitut, Universitat Bayreuth, 95447 Bayreuth, Germany, ³EPFL, CH-1015, Lausanne, Switzerland, ⁴Tohoku University, Sendai 980-8578, Japan, ⁵Institute of Geochemistry, CAS, Guiyang, China, ⁶National Astronomical Observatories, CAS, Beijing, China, ⁷Guangzhou Institute of Geochemistry, CAS, Guangzhou, China, ⁸National Institute of Polar Research, Tokyo, Japan

Introduction: Exploration for paleoenvironment and possible existence of life on Mars are the main goals of Mars missions. Martian meteorites, the only available rocks from Mars, supply us with a unique chance to study these issues using various sophisticated instruments. Tissint is a new witnessed Martian meteorite fall. The unique fresh samples of Tissint are critically important for study of organic compounds in Martian meteorites, since terrestrial contamination is a very serious issue. Tissint is an olivine-phyric shergottite, consisting mainly of olivine phenocrysts, maskelynite (shocked glass of plagioclase) and pyroxenes with minor chromite, ilmenite, sulfide and apatite [1,2]. The meteorite has been heavily shocked, as indicated by presence of shock-melt veins and pockets, maskelynite and various high-pressure assemblages [2,3]. At least 3 shock events were recognized in Tissint [3]. Here we report discovery of organic carbon in this meteorite and the in situ element and isotope analyses. Our observations favor for a biogenic origin.

Results: The organic carbon has two petrographic settings, most fully filling fractures and cleavages in olivine and pyroxenes and a few enclosed in the shock-melt veins. Laser micro-Raman analysis shows that the organic carbon is similar to kerogen. Furthermore, a sharp peak at 1327 cm⁻¹ was detected in some organic carbon inclusions in the shock-melt veins, indicative of formation of diamond by a shock event. The organic carbon of both petrographic settings has been analyzed with the Cameca NanoSIMS 50L. The elemental ratios of H, N, O, S, P and Cl to C of the organic carbon are comparable with the working reference of coal, but distinctly higher than the graphite standards, confirming that the organic carbon is a kerogen-like matter. Except for 4 grains with normal H isotopes, all other 9 analyses are highly D-enriched ($\delta D = 324 \sim 1183$ permil). The organic carbon is characteristic of light C isotopes, with $\delta^{13}C$ values of $-13.0 \sim -33.3$ permil. The N isotopes are normal within the analytical uncertainty.

Discussion and Conclusions: The presence in the shock-melt veins and the D-enrichment of the organic carbon demonstrate a Martian origin. Furthermore, the clear petrographic settings of the organic carbon evidently indicate depositing from organic fluids, after eruption of Tissint basalt and the following shock event that produced abundant fractures. The organic carbon cannot be magmatic in origin claimed by previous work, which was based on its presence in mis-described "magmatic inclusions" [4]. The organic carbon is either unlikely derived from chondritic debris that impacted on Mars, because kerogen is an insoluble organic matter. The significantly light C isotopes of the organic carbon suggest a biogenic origin. Our observations are the currently available evidence for possible biotic activity on Mars.

References: [1] Aoudjehane H. C., et al. 2012. *Science* 338: 785-788. [2] Lin Y. T., et al. 2012. *Meteoritics & Planetary Science* 75: 5131. [3] El Goresy A., et al. 2013. *Lunar and Planetary Science Conference XXXIV*: #1037. [4] Steele A., et al. 2012. *Science* 337: 212-215.

キーワード: Mars, meteorite, Life, organic carbon, isotopes, SIMS
Keywords: Mars, meteorite, Life, organic carbon, isotopes, SIMS

Evidence for a dynamic event recorded in HED meteorites Evidence for a dynamic event recorded in HED meteorites

宮原 正明^{1*}, 大谷 栄治¹, 山口亮², 小澤 信², 境 毅³, 平尾 直久⁴

Masaaki Miyahara^{1*}, Eiji Ohtani¹, Akira Yamaguchi², Shin Ozawa², Takeshi Sakai³, Hirao Naohisa⁴

¹Graduate School of Science, Tohoku University, ²National Institute of Polar Research, ³Geodynamics Research Center, Ehime University, ⁴Japan Synchrotron Radiation Research Institute

¹Graduate School of Science, Tohoku University, ²National Institute of Polar Research, ³Geodynamics Research Center, Ehime University, ⁴Japan Synchrotron Radiation Research Institute

It is expected that HED meteorites originate from one of the largest asteroids in the solar system, 4 Vesta. Recent Dawn mission operated by NASA also supports the prediction [1][2]. Dawn mission clearly revealed the existence of many craters on 4 Vesta, which are the records of heavy meteorite bombardments. The existence of a high-pressure polymorph in a shocked meteorite is a robust evidence for a dynamic event on its parent-body (e.g., [3][4]). A high-pressure polymorph can be used for estimating the magnitude of a dynamic event (e.g., [5][6]). Some previous studies propose that 4 Vesta might suffer from late heavy bombardment (LHB) as well as the moon [7]. However, a high-pressure polymorph has not been found in HED meteorite so far.

We got one of eucrite samples, Bereba to clarify a dynamic event occurred on 4 Vesta using a high-pressure polymorph. Present Bereba sample has several shock-melt veins, implying that it was heavily shocked. Accordingly, we investigated Bereba using Raman spectroscopy, FEG-SEM, synchrotron(s)-XRD and FIB-TEM techniques to clarify a record of a dynamic event occurred on 4 Vesta.

We focused our interest on silica phase in this study. Raman spectroscopy analyses show that the silica grains in the host-rock of Bereba are cristobalite, tridymite and quartz. Most quartz grains entrained in the shock-melt veins are partly replaced with coesite. BSE images show that silica grains entrained in or adjacent to the shock-melt veins have network-like and/or lamellae-like textures. Raman spectroscopy, s-XRD analyses and TEM images indicate that such silica grains include coesite, stishovite and silica glass along with quartz.

We found the high-pressure polymorphs of silica from HED meteorites for the first time. The existence of stishovite indicates that pressure condition recoded in Bereba should be ~8 GPa at least based on a phase diagram obtained from static high-pressure and high-temperature synthetic experiments [8]. Two giant impact basins on 4 Vesta are depicted by Dawn mission. Crater chronology obtained by Dawn mission reveals that the giant impact basins were formed around 1.0 Ga ago [9]. Its fragments became Vesta family in asteroid belt, and a part of them fell into the Earth as HED meteorites. The existence of high-pressure polymorphs in Bereba may support the giant impact occurred on 4 Vesta

References:

[1] De Sanctis M.C. et al. (2012) *Science*, 336, 697-700. [2] Russell C.T. et al. (2012) *Science*, 336, 684-686. [3] Ohtani E. et al. (2011) *PNAS*, 108, 463-466. [4] Miyahara M. et al. (2011) *PNAS*, 108, 5999-6003. [5] Chen M. et al. (1996) *Science*, 271, 1570-1573. [6] Ohtani E. et al. (2004) *EPSL*, 227, 505-515. [7] Bogard D.D. (2011) *Chem. Erde.*, 71, 207-226. [8] Zhang J.R.C. et al. (1993) *J. Geophys. Res.* 98, 19785-19793. [9] Marchi S. et al. (2012) *Science*, 336, 690-694.

放射光マイクロ XANES 分析による集積岩ユークライト Y-75011 と表層ユークライト Y 980433 中斜長石の鉄の価数分析 Iron valences of plagioclase from cumulate eucrites Y-75011 and surface eucrite Y 980433 as inferred from micro-XANES an

佐竹 渉^{1*}, ポール ブキャナン², 武田 弘¹, 三河内 岳¹, 宮本 正道¹
Wataru Satake^{1*}, Paul C. Buchanan², Hiroshi Takeda¹, Takashi Mikouchi¹, Masamichi Miyamoto¹

¹ 東京大学大学院理学系研究科地球惑星科学専攻, ² キルゴア大学

¹Department of Earth and Planetary Science, Graduate School of Science, University of Tokyo, ²Kilgore College

The HED (Howardites, Eucrites and Diogenites) meteorites are the largest group of achondrites and are widely believed to have originated on 4Vesta. Eucrites are mainly composed of pyroxene and plagioclase, and are considered to have been derived from the crust of the asteroid. Recently, the Dawn spacecraft observation has revealed the existence of a metallic core in Vesta and that it experienced early differentiation in the solar system. In this way, Vesta is an important example of early differentiation in the solar system, and thus, HED meteorites may offer substantial information to understand igneous differentiation on Vesta.

The oxidation state of magmas is one of the most significant factors in controlling mineral crystallization and is relevant to the redox state of the parent body. In our previous study, we estimated redox states of six eucrites by using synchrotron radiation (SR) Fe XANES measurement of plagioclase. This study reveals that the $\text{Fe}^{3+}/(\text{Fe}^{2+} + \text{Fe}^{3+})$ ratios of plagioclase in cumulate eucrites are higher than those of surface eucrites, which indicates that the deep crust of Vesta was a relatively more oxidized environment. However, this result needs to be reassessed by analyzing minimally metamorphosed samples because most eucrites have experienced significant degrees of thermal metamorphism.

In this study, we focused on surface and cumulate eucrites that were not affected by annealing, in order to compare the XANES results with our previous study.

We analyzed thin sections of surface eucrite clast in Y-75011 and cumulate eucrite Y 980433. We first carefully observed them by optical and scanning electron microscopes, and analyzed them by electron microprobe in order to select representative plagioclase grains for SR Fe-XANES. SR Fe-XANES was performed at BL-4A, Photon Factory, KEK, Tsukuba, Japan to measure $\text{Fe}^{3+}/(\text{Fe}^{2+} + \text{Fe}^{3+})$ ratios of plagioclase. The SR beam size was about 5×6.5 micro meter. The XANES analyses for standard kaersutites with known $\text{Fe}^{3+}/(\text{Fe}^{2+} + \text{Fe}^{3+})$ ratios shows a linear relationship between centroid energy position of XANES pre-edge spectra and the $\text{Fe}^{3+}/(\text{Fe}^{2+} + \text{Fe}^{3+})$ ratio. Based on this linear relationship, we estimated the $\text{Fe}^{3+}/(\text{Fe}^{2+} + \text{Fe}^{3+})$ ratio of samples.

Optical and scanning electron microscope observations show that all samples are mainly composed of pyroxene and plagioclase. The plagioclase abundance in Y-75011 is about 30 vol. % and Y 980433 is about 50 vol. %, respectively. All plagioclase grains analyzed display clear pre-edge peaks in the obtained XANES spectra. The $\text{Fe}^{3+}/(\text{Fe}^{2+} + \text{Fe}^{3+})$ ratio of Y-75011 is estimated to be 0.10-0.14 and Y 980433 is 0.48-0.58, respectively.

The $\text{Fe}^{3+}/(\text{Fe}^{2+} + \text{Fe}^{3+})$ ratios of plagioclase in two eucrites studied show contrasting values (0.12 vs. 0.52). The $\text{Fe}^{3+}/(\text{Fe}^{2+} + \text{Fe}^{3+})$ ratio of the Y-75011 surface eucrite is consistent with our previous study of other surface eucrites (Padvarninkai, ALH 76005, Piplia Kalan and Petersburg) in its low $\text{Fe}^{3+}/(\text{Fe}^{2+} + \text{Fe}^{3+})$ ratio. Similarly, the $\text{Fe}^{3+}/(\text{Fe}^{2+} + \text{Fe}^{3+})$ ratio of the Y 980433 cumulate eucrite is consistent with our previous study of other cumulate eucrites (EETA 87520 and Moore County).

This study demonstrated that the $\text{Fe}^{3+}/(\text{Fe}^{2+} + \text{Fe}^{3+})$ ratios of plagioclase from surface and cumulate eucrites have not been affected by later thermal metamorphism, and they are likely to reflect the redox state of the crystallization environment. Thus, we suggest that there was a heterogeneous redox environment in Vesta, where surface areas were more reduced than the crust and deep interior.

There are two possible scenarios for explaining these features. One is that the oxidizing environment of Vesta's deep crust was caused by water in Vesta's interior. The other possibility is that the oxidized environment was originally related to the early differentiation of Vesta. Although we cannot determine which model is more likely at present, this study at least reveals Vesta's deep crust shows a global oxidized environment.

キーワード: XANES, ユークライト, ベスタ, 斜長石

Keywords: XANES, Eucrite, Vesta, Plagioclase

カルシウムに富む斜長石の分化した隕石母天体と月における形成分解過程と地球環境の考察

Formation of Ca-rich Plagioclase in Meteoritic and Lunar Crust and its Decomposition with Reference to Earth Environment

武田 弘^{1*}, 長岡 央², 唐牛 謙³, 大竹 真紀子³, 矢沢 勇樹⁴, 山口 亮⁵, 三河内 岳¹

Hiroshi Takeda^{1*}, Hiroshi Nagaoka², Yuzuru Karouji³, Makiko Ohtake³, Yuuki Yazawa⁴, Akira Yamaguchi⁵, Takashi Mikouchi¹

¹ 東京大学理学系研究科地球惑星科学専攻および千葉工大フォーラム研究, ² 早稲田大学, ³ 宇宙科学研究所, ⁴ 千葉工大生命環境科学, ⁵ 国立極地研究所

¹ Univ. of Tokyo, Graduate School of Science, ² Waseda Univ., ³ JAXA/ISAS, ⁴ Chiba Inst. of Tech., Dept. of Life & Environm. Sci., ⁵ National Inst. of Polar Res.

最近の「かぐや」による月探査と、Dawn 探査機による小惑星ベスタの探査、「はやぶさ」の採取した LL コンドライト試料に関連した研究により、始原的な地殻を持つ小天体の物質分布とその形成過程が明らかになりつつある。これよりコンドライト的始原物質が、母天体での内部加熱と衝突による部分溶融により生ずるグラニュライト的物質には、アルバイトとダイオプサイトよりなる安山岩的物質が部分的に形成されていることが判明した [1,2,3]。しかし、これよりもっと大きな隕石母天体であるベスタでは、表面近くにマグマ大洋が形成され、カルシウムに富む斜長石とピジョン輝石よりなるユークライトが形成され、その下の下部地殻には斜方輝石のみからなるダイオジェナイトがあるという層状地殻モデルが我々により提唱されていた [6]。最近の Dawn 探査機による小惑星ベスタの探査 [5] により、このモデルが実証された [5]。日本の「かぐや」月探査機により、月裏側高地にはトリウムの最も少なく Mg number の高い苦鉄質ケイ酸塩鉱物を極少量含む純粋に近いカルシウムに富む斜長石よりなる原始地殻が残っている可能性のある地域が確認された。月の裏側にある大きな盆地は月初期にできて以後、表側のように溶岩により満たされることなく、古い地形が未だに残っている。この月裏側について、「かぐや」の得た大きな成果である重力分布図、地形カメラ (TC), マルチバンドイメージャ (MI), レーザ光度計 (LALT) により地形図、地殻の厚さの分布図、ガンマ線分光計 (KGRS) によるトリウム分布図 [8] より、地殻がもっとも厚く、トリウムの最も少ない地域が発見された。また MI, スペクトルプロファイラ (SP) より [9] アポロ試料の斜長岩より、より始原的な月地殻が残っている可能性が高いと考えられる。月の裏側から来たと思われる月隕石、ドーファー 489, 307, 309 月隕石の鉱物学的、地球化学的研究より、この地域にあるデリクレ-ジャクソン・ベースン (FS-DJ) 底で形成された可能性も示された [10]。アポロ計画で持ち帰られた斜長岩の研究より通説となっていたマグマ大洋モデルでは説明がつかない事実が増えている。コンドライト的始原物質の部分溶融によるマグマ大洋から、ベスタのようなカルシウムに富む斜長石を晶出するマグマ大洋をつくるには、マグマ大洋への隕石様小天体の衝突によりナトリウムを気化して追い出すようなモデル [7] も提唱されている。月のカルシウムに富む純粋に近い斜長岩を晶出するモデル [9] には、月のジャイアント・インパクト・モデルによるナトリウムの消失も関与している。カルシウムに富む純粋に近い斜長石は森林土壌でつくられるフルボ酸で容易に分解されるので、地球上ではそのカルシウムが川により海に運ばれ、炭酸ガスをウーライトのような炭酸カルシウムとして沈殿することが考えられるので、このような炭酸ガス固定も地球の環境問題を考える時に考慮しなくてはならないだろう。

引用文献： 英文参照

キーワード: 月裏側, 月隕石, 月地殻, かぐや探査機, ベスタ, LL コンドライト

Keywords: Lunar farside, lunar meteorites, lunar crust, Kaguya mission, Vesta, LL chondrite.

Petrology and mineralogy of a new polymict ureilite Yamato 983890 Petrology and mineralogy of a new polymict ureilite Yamato 983890

小澤 信^{1*}, 山口 亮¹, 小島 秀康¹
Shin Ozawa^{1*}, Akira Yamaguchi¹, Hideyasu Kojima¹

¹National Institute of Polar Research, Tokyo 190-8518, Japan

¹National Institute of Polar Research, Tokyo 190-8518, Japan

Introduction

Ureilites are the second largest group of achondrites. They are largely divided into two types: monomict and polymict. More than 90 % of ureilites are monomict ureilites, whereas polymict ureilites are relatively rare with only 23 approved meteorites [1]. Polymict ureilites are polymict breccias composed of lithic clasts and mineral fragments of various lithologies, some of which are unlike monomict ureilites [2-5]. Therefore, polymict ureilites provide valuable information about igneous and collisional processes on ureilite parent bodies, which cannot be extracted from monomict ureilites. Yamato (Y-) 983890 is a recently classified polymict ureilite [6]. In this study, we conducted careful petrographic observations on this new polymict ureilite.

Results and Discussions

Y-983890 consists of lithic clasts and mineral fragments which show a large variety of lithologies. Most of them are monomict ureilite-like materials, but some are not. The non-monomict ureilite-like materials include feldspathic clasts, dark clasts (carbonaceous chondrite-like), a chondrule/chondrite fragment, and others.

Monomict ureilite-like clasts/mineral fragments

The monomict ureilite-like clasts/mineral fragments in Y-983890 consist of coarse-grained (up to 1 mm) olivine and/or pyroxene with interstitial dark carbonaceous materials and/or graphite. Olivine has a chemical composition of Fo₇₄₋₉₆ with high CaO (0.26-0.46 wt%) and Cr₂O₃ (0.47-0.91 wt%) contents. Pyroxene is mainly pigeonite (En₇₂₋₈₇Wo₅₋₁₁) and orthopyroxene (En₇₉₋₈₅Wo₂₋₅), but minor augite (En₅₅₋₆₄Wo₃₃₋₃₉) is also present. Chemical compositions of olivine and pyroxene, and Fe/Mg-Fe/Mn relations of olivine are consistent with those of monomict ureilites [4, 7].

Feldspathic clasts

Since monomict ureilites do not contain feldspar, lithic clasts containing feldspar are considered to be of non monomict-ureilite origin. We identified several distinct feldspathic clasts. They show different igneous textures and chemical compositions of constituent minerals (feldspar and pyroxene). Most feldspar has albitic compositions (Ab₈₀₋₈₇Or₃₋₈), but more An-rich one (Ab₅₅Or₆) is also present in a clast. Pyroxene is mostly augite (En₄₀₋₆₂Wo₂₁₋₃₈) and some clasts contain enstatite (En₁₀₀, En₆₇Wo₄) and pigeonite (En₃₈Or₁₅). These feldspathic clasts could be basaltic counterparts complementary to monomict ureilites (=ultramafic residues or cumulate).

Dark clasts (carbonaceous chondrite-like)

Y-983890 contains a lot of dark clasts. They mainly consist of fine-grained phyllosilicate-rich matrices with variable amounts of opaque minerals such as magnetite and sulfides. Magnetite occurs as spherical or framboidal grains, or as irregular aggregates. Sulfides such as pyrrhotite and pentlandite occur as euhedral crystals or anhedral polycrystalline aggregates. These dark clasts mineralogically resemble the matrices of CI carbonaceous chondrites.

Chondrule/chondrite fragment

A chondrule fragment was identified in Y-983890. It shows a barred olivine chondrule texture, consisting of barred olivine crystals (Fo₇₉₋₈₂) with interstitial devitrified mesostasis with albitic composition (Ab₈₃Or₉). The chemical composition of the olivine is in the range of that of H chondrite

The dark clasts and the chondrule/chondrite fragment are considered to be fragments of impactors collided with ureilite parent bodies.

References

- [1] Meteoritical Bulletin Database (<http://www.lpi.usra.edu/meteor/metbull.php>)
- [2] Ikeda Y. et al. (2000) Antarctic Meteorite Research, 13, 177-221.

Japan Geoscience Union Meeting 2013

(May 19-24 2013 at Makuhari, Chiba, Japan)

©2013. Japan Geoscience Union. All Rights Reserved.



PPS02-07

会場:203

時間:5月20日 11:15-11:30

[3] Ikeda Y. et al. (2003) Antarctic Meteorite Research, 16, 105-127.

[4] Goodrich C. A. et al. (2004) Chemie der Erde, 64, 283-327.

[5] Cohen B. A. et al. (2004) Geochimica et Cosmochimica Acta, 68, 4249-4266.

[6] Yamaguchi A. et al. (2012) Meteorite Newsletter, 21. (http://yamato.nipr.ac.jp/AMRC/AMRC/MeteoriteNewsletter_21.pdf)

[7] Goodrich C. A. (1992) Meteoritics, 27, 327-352.

Keywords: ureilite, polymict, breccia, Yamato (Y-) 983890

ユレイライト隕石中のダイヤモンド：生成メカニズムと惑星過程での役割 Diamond in ureilites: Formation mechanisms and roles in planetary processes

中牟田 義博^{1*}Yoshihiro Nakamuta^{1*}¹九州大学総合研究博物館，九州大学¹Kyushu University Museum, Kyushu Univ.

Diamond was found in the Novo Urei meteorite, one of typical ureilites, first in meteorites in 1888. Lonsdaleite, hexagonal polymorph of diamond, was found in the Canyon Diablo iron and the Goalpara ureilite first in nature. So far, mineralogical properties of carbon minerals in ureilites have been only roughly determined by using acid-treatment residues because they exist in small quantities in ureilites. Then, the origin of diamonds in ureilites has been controversial.

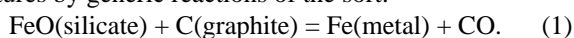
We observed carbon minerals under an optical microscope under a reflected light and obtained micro Raman spectra of them in polished thin sections. X-ray powder diffraction patterns were obtained from the carbon grains directly taken out of polished thin sections and picked up from disaggregated ureilite samples. Carbon minerals in these carbon grains were also directly observed by TEM and SEM.

In weakly shocked ureilites, diamond occurs with a granular shape of up to a few micron meters in size and shows sharp x-ray diffraction lines and sharp Raman bands at 1332 cm^{-1} , suggesting well-crystallinity of them. Lonsdaleite was not found in weakly shocked ureilites. In heavily shocked ureilites, diamond occurs together with lonsdaleite with a platy shape of up to a few tens micron meters in size and shows very broad x-ray diffraction lines and broad Raman spectra.

Selected area electron diffraction analyses and high resolution TEM observations of carbon grains from the heavily shocked Goalpara ureilite reveal the relative crystal-axes orientations between graphite (Gr), lonsdaleite (Lo) and diamond (Di) as $(001)_{Gr} // (100)_{Lo} // (111)_{Di}$, $[210]_{Gr} // [001]_{Lo} // [2-1-1]_{Di}$ and $(1-20)_{Gr} // (-120)_{Lo} // (0-22)_{Di}$. The shapes of diffraction spots in the SAED patterns reveal that the transformation of graphite to lonsdaleite and diamond is initiated by sliding of hexagonal carbon planes of graphite along the $[210]$ of graphite structure. These results suggest that lonsdaleite and diamond in heavily shocked ureilites formed directly from graphite through boat-type buckling and chair-type puckering of hexagonal carbon planes of graphite, respectively¹.

A SEM image of the surface parallel to the basal plane of original graphite from the weakly shocked Y-8448 ureilite is shown in Figure 1. In the figure, triangular crystal faces were observed. BSED patterns reveal that the triangular faces correspond to $(1\ 1\ 1)$ crystal planes of diamond. Such forms of diamond clearly reveal that the diamond crystals have grown on the melt and strongly suggest that diamond in the weakly shocked ureilites was formed through catalytic processes.

In the planetary processes of the ureilite parent body, smelting is thought to be an important process by which the chemical structure of the body was controlled. Ferrous silicates are vulnerable to smelting in the presence of graphite at magmatic temperatures by generic reactions of the sort:



On as much as gas of large molar volume appears only on the right-hand side of this reaction, the reaction is expected to be strongly pressure sensitive. Smelting is suppressed at elevated pressure and promoted as pressure falls². Then, mg# of olivine is controlled by the depth at which it has been crystallized. In order to confirm the reaction (1) and the smelting process in the ureilite parent body, it is important to know the relation between mg# of silicate and the modal abundance of carbon. The modal abundance of original graphite in ureilites was obtained under an optical microscope (Figure 2). Figure 2 shows that the modal abundance of carbon decreases with the increase of mg# and directly confirms the reaction (1) and the smelting process in the ureilite parent body.

¹ Nakamuta and Toh (2013) Amer. Mineral., in press; ² Walker and Grove (1993) Meteoritics 28, 629.

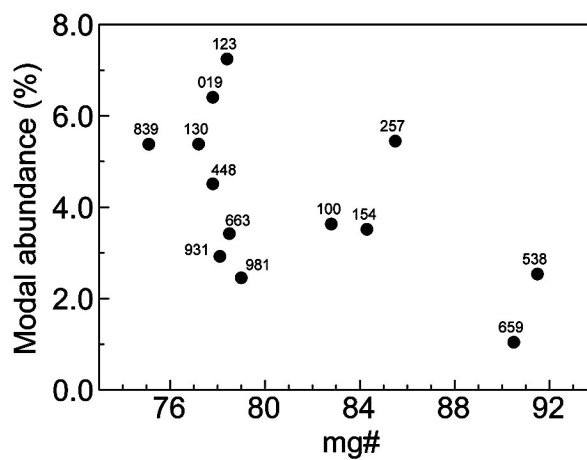
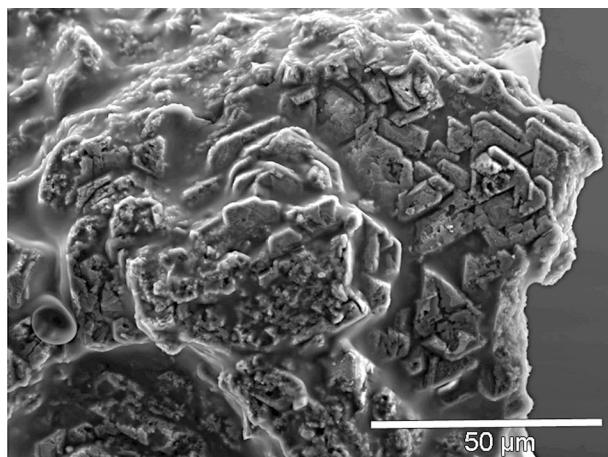
キーワード: ユレイライト隕石, ダイヤモンド, ロンスデル石, グラファイト, 相転移

Keywords: ureilite, diamond, lonsdaleite, graphite, transformation

PPS02-08

会場:203

時間:5月20日 11:30-12:00



Shisr 007 ユレーライトの炭素質物質中の不均一希ガス分布 Heterogeneous distribution of noble gases in carbonaceous materials of Shisr 007 Ureilite

安藤高太郎², 岡崎隆司², 中村 智樹^{1*}
ANDO Koutaro², OKAZAKI Ryuji², Tomoki Nakamura^{1*}

¹九州大学, ²東北大学

¹Kyushu University, ²Tohoku University

We have characterized carbonaceous materials in Shisr 007 ureilite by multidiscipline techniques for mineralogy and noble gas signatures to gain better understandings of the differentiation process of ureilite parent body and the formation mechanism of carbonaceous materials.

Optical microscope observation revealed that Shi.r 007 is an olivine-pigeonite type monomict ureilite. The olivine shows undulatory extinction and planar deformation fractures, corresponding to shock stage S3 (Shock pressure <20GPa). EPMA analysis showed that core composition of olivine (Fo=79) and pyroxene (En=73) in Shisr 007 are close to the average composition of silicates in ureilites and therefore Shisr 007 formed via differentiation process similar to other ureilites.

Diamond, graphite, and compressed graphite, which is an intermediate phase formed during graphite-diamond phase transition, are identified in carbonaceous materials by SR-XRD. Shisr 007 contains a large carbonaceous material (BCM; 1000 x 1500 microns on a polished section). It has rectangular, blade-like shape,

implying that it was a large single crystal of graphite, as is observed in ALH 78019. Using an edged tool, BCM was separated into small pieces typically 200-300 micron in diameter. A amoeboid-shape carbonaceous materials (ACM; typically 100-400 micron in size) commonly occur and were separated from the polished section with HF/HCl. Individual 17 pieces of the BCM were first measured with Si-std by synchrotron X-ray diffraction (SR-XRD) to determine their diamond abundances. The data show that diamond abundance is roughly proportional to the weight. After the SR-XRD analyses, noble gas compositions of 10 ACMs and 16 BCMs were analyzed by stepwise heating method (600, 1300, 1900, and 2100C) using Pot-pie furnace designed for small sample analysis. In addition, 2 samples of BCMs are measured in 6 steps adding 1000 and 1600C fraction. The ACMs have relatively constant ³⁶Ar contents (30-200 x 10⁻⁶ccSTP/g) and ³⁶Ar/¹³²Xe elemental ratios (100-200), while BCMs show a wider range of ³⁶Ar contents (3-400 x 10⁻⁶ccSTP/g) and a higher ³⁶Ar/¹³²Xe ratios (150-450). A major part (70-95%) of primordial ³⁶Ar, ⁸⁴Kr, and ¹³²Xe was released at 1600-2100C fraction. To identify where the carrier of noble gases are, we performed the heating experiment of CVD diamond synthesized by the hot filament method. CVD diamonds were started to decompose at 1600C, confirmed by their Raman spectra and microscopic observation, which is consistent that the main gas carrier phase of Shisr 007 is diamond. However, diamond abundances and gas concentrations did not correlated, indicating that diamonds have variable gas contents: Some diamonds contain large amounts of noble gases, but the other diamonds are almost free of gases. The heterogeneous noble gas compositions of the BCMs and ACMs imply that they have formed from multiple stages of thermal and shock metamorphism.

キーワード: ユレーライト, 希ガス

Keywords: Ureilite, Noble gases

Reduction, oxidation and sulfidation in ordinary, enstatite and R chondrites based on speciation of iron Reduction, oxidation and sulfidation in ordinary, enstatite and R chondrites based on speciation of iron

Timothy Fagan^{1*}

Timothy Fagan^{1*}

¹Department of Earth Sciences, Waseda University, Tokyo, Japan

¹Department of Earth Sciences, Waseda University, Tokyo, Japan

Speciation of iron plays the pivotal role in distinguishing the H, L, LL groups of ordinary (O) chondrites and O vs. enstatite (E) and R chondrites [1,2]. The variations in Fe-bearing minerals among these chondrite groups reflect variable physical conditions from different locations and times in the inner solar nebula. Most previous work has focused on speciation of Fe between silicates and metals as an indicator of oxygen vs. reduction [e.g., 1,2]. This project considers the role of sulfidation as well as reduction and oxidation in chondrite-forming regions of the solar nebula.

This approach depends on determining the speciation of Fe between silicates, metallic minerals and sulfides (mostly troilite). Data set (1) is based on modes and mineral compositions from thin sections of H, L, LL, E and R chondrites. These include: Ben-sour (LL6, fall); Mt. Tazerzite (L5, fall); Tamdakht (H5, fall); St. Marks (EH5, fall); Lewis Cliff 88180 (EH5, find); Northwest Africa 974 (E6, find); Northwest Africa 753 (R3, find). Meteorite falls and type 5 and 6 chondrites were emphasized in order to minimize heterogeneity of mineral compositions and effects of terrestrial weathering. In Data (1), modes were determined from manual counting of grids overlain on elemental maps, and mineral compositions were determined using a JEOL JXA-8900 electron microprobe at Waseda University. Data set (2) is based on whole-rock wet chemical analyses conducted and compiled by E. Jarosewich [3,4]. We used falls for LL (n = 17), L (n = 57) and H (n = 31) and all of the E (1 fall, 3 finds) chondrites from the Jarosewich compilation. Data set (3) is based on similar whole-rock analyses conducted by H. Haramura of NIPR and compiled by Yanai and Kojima [5]. This data set consists of Antarctic finds (59 LL, 158 L, 162 H, 6 E).

This project also requires an understanding of reactions that transfer Fe between the silicate, sulfide and metal subsystems within whole-rock reacting systems of O, E and R chondrites. A reaction space [6,7] approach was used to identify the main reactions that change mineral abundances in these rocks: (R1) $\text{NaAlSi}_3\text{O}_8 = \text{NaAlSi}_2\text{O}_6 + \text{SiO}_2$; (r2) $\text{Mg}_2\text{SiO}_4 + \text{SiO}_2 = 2 \text{MgSiO}_3$; (R3) $\text{FeSiO}_3 = \text{Fe-metal} + \text{SiO}_2 + 0.5\text{O}_2$; (R4) $\text{FeSiO}_3 + 0.5 \text{S}_2 = \text{FeS} + \text{SiO}_2 + 0.5 \text{O}_2$. R1 does not appear to be important in most chondrites. R2 is very important as it describes variations in abundance of olivine vs. pyroxene, but this reaction occurs entirely within the silicate subsystem. Reduction of Fe occurs with progress on R3, so forward progress on R3 can be estimated from the ratio of metallic Fe to all Fe, and can be used as a monitor of reduction. Likewise, forward progress on R4 can be used as a monitor of sulfidation. In this framework, if $R3 = 1$, all Fe occurs as Fe-metal; if $R4 = 1$, all Fe occurs as Fe-sulfide; if $R3 = R4 = 0$, all Fe occurs as FeO in silicates.

The three data sets all show a wide range of reduction and little variation in sulfidation for O chondrites ($R3$ from 0 to 0.7; $R4 \sim 0.2$). E chondrites appear to be more reduced and sulfidized ($R3$ from 0.7 to 0.8; $R4$ from 0.2 to 0.3). The R chondrite of this study is oxidized and somewhat sulfidized ($R3 = 0$; $R4 \sim 0.3$). Most deviations from these patterns occur in Data (3) and are probably due to terrestrial weathering. Results suggest that an oxidant (or reductant) was independent of sulfur fugacities in the regions where ordinary chondrites formed.

[1] van Schmus W.R. and Wood J.A. (1967) GCA 31: 747-765. [2] Weisberg M.K. (2006) in Lauretta D.S. and McSween H.Y. Jr. (editors) Meteorites and the Early Solar System II, p. 19-52. [3] Jarosewich E. (1990) MaPS 31: 323-337. [4] Jarosewich E. (2006) MaPS 41: 1381-1382. [5] Yanai K. and Kojima H. (1995) Catalog of the Antarctic Meteorites, National Institute of Polar Research, 230 p. [6] Thompson J.B. Jr. et al. (1982) J. Petrol. 23: 1-27. [7] Fagan T.J. and Day H.W. (1997) Geology 25: 395-398.

キーワード: chondrites, oxygen fugacity, sulfur fugacity, solar nebula

Keywords: chondrites, oxygen fugacity, sulfur fugacity, solar nebula

角礫岩 LL コンドライトに含まれるアルカリに富む岩片の K-Ca 同位体年代学 K-Ca systematics of alkali-rich fragments in LL-chondritic breccias

横山 立憲^{1*}, 三澤 啓司², 岡野修³, Chi-Yu Shih⁴, Laurence E. Nyquist⁵, Justin I. Simon⁵, Michael J. Tappa⁴, 米田 成一⁶
Tatsunori Yokoyama^{1*}, Keiji Misawa², Osamu Okano³, Chi-Yu Shih⁴, Laurence E. Nyquist⁵, Justin I. Simon⁵, Michael J. Tappa⁴, Shigekazu Yoneda⁶

¹ 総合研究大学院大学, ² 国立極地研究所, ³ 岡山大学・理, ⁴ ESCG/Jacobs Technology, ⁵ NASA Johnson Space Center, ⁶ 国立科学博物館理工学研究部

¹ SOKENDAI, ² NIPR, ³ Okayama Univ., ⁴ ESCG/Jacobs Technology, ⁵ NASA Johnson Space Center, ⁶ NMNS

Introduction: Alkali-rich fragments in LL-chondritic breccias, Kraehenberg, Bhola and Y-74442 are very similar in mineralogy and petrography, suggesting that they could have come from related precursor materials [1,2]. Recently we reported Rb-Sr isotopic systematics of alkali-rich igneous rock fragments in Y-74442 [2]. The extremely high Rb/Sr value (2.58 at 4.429 Ga ago) of this source can be explained by mixing of a chondritic component with an alkali-rich component formed in the early solar nebula. Since alkali-rich fragments in the LL-chondritic breccias are highly enriched in K, we can expect enhancements of radiogenic ⁴⁰Ca. The decay of ⁴⁰K to ⁴⁰Ca has not been widely used for dating due to the high abundance of ⁴⁰Ca along with the fractionation of Ca isotopes during analysis in the mass spectrometer. Here, we report preliminary results of K-Ca isotopic systematics of alkali-rich fragments in Y-74442.

Results and Discussion: The Ca abundances in samples were calculated from their ⁴⁸Ca/⁴⁴Ca ratios, normalized to ⁴²Ca/⁴⁴Ca = 0.31221 [3]. While the Ca abundances in alkali-rich fragments of Y-74442 are almost constant and chondritic (1.3-1.8 x CI), the fragments show enrichments of K (5-15 x CI) [2]. Over time, the enrichment of K in alkali-rich fragments of Y-74442 result in large epsilon ⁴⁰Ca values (epsilon ⁴⁰Ca = 2-7) relative to other planetary materials [4,5]. The data of Y-74442 fragments yield a K-Ca age of 4.51 +/- 0.23 Ga (2 sigma, MSWD = 3.5, n = 6) for lambda (⁴⁰K) = 0.5543 Ga⁻¹ [6,7] with an initial ⁴⁰Ca/⁴⁴Ca = 47.1587 +/- 0.0032 (2 sigma) using the Isoplot/Ex program [8]. Since K-Ca data for one fragment of Y-74442 deviates from the isochron, we exclude the data from the calculation. This age is within error of the previously reported Rb-Sr age of 4.429 +/- 0.054 Ga [2]. We could obtain a mean initial ⁴⁰Ca/⁴⁴Ca ratio of 47.1597 at 4.429 Ga (the more reliable Rb-Sr age). Then, using the initial ⁴⁰Ca/⁴⁴Ca value of bulk silicate earth at 4.568 Ga, the source ⁴⁰K/⁴⁴Ca ratio of 0.00162 for the fragments is obtained. This source for alkali-rich fragments is about 4.5 times higher than that of the LL-chondrite parent body (⁴⁰K/⁴⁴Ca = 0.00035) [9]. It is consistent with the Rb-Sr systematics of Y-74442 fragments [2] and suggesting that the K enrichment may have also occurred by vapor/solid (or liquid) fractionations in the early solar system. A mixture of the alkali component (early nebular condensates) and the ferromagnesian component could reflect flash heating induced by impact on an LL chondritic parent body at least 4.429 Ga ago, and further enrichments of K and Rb relative to Ca and Sr, respectively, could have occurred during this event. The resulting impact-melt rocks could have been fragmented by later impact event(s) and finally incorporated into the Y-74442 parent body.

References: [1] Wlotzka F. et al. (1983) *Geochim. Cosmochim. Acta* 47, 743. [2] Yokoyama T. et al. (2013) *Earth Planet. Sci. Lett.* doi: 10.1016/j.epsl.2013.01.037, in press. [3] Russell W. A. et al. (1978) *Geochim. Cosmochim. Acta* 42, 1075. [4] Caro G. et al. (2010) *Earth Planet. Sci. Lett.* 296, 124. [5] Simon J. I. et al. (2009) *Astrophys. J.* 702, 707. [6] Marshall B. D. & DePaolo D. J. (1982) *Geochim. Cosmochim. Acta* 46, 2537. [7] Steiger R. H. & Jaeger E. (1977) *Earth Planet. Sci. Lett.* 36, 359. [8] Ludwig K. R. (2009) *Spec. Publ.*, vol. 2, Berkeley Geochronol. Cent., Berkeley, Calif. [9] Wasson J. T. & Kallemeyn G. W. (1988) *Phil. Trans. R. Soc. Lond. A* 325, 535.

キーワード: コンドライト, アルカリ元素, 年代学
Keywords: chondrite, alkaline elements, chronology

始原的なメソシデライト NWA 1878 A primitive mesosiderite NWA 1878

杉浦 直治^{1*}, 木村真²
naoji sugiura^{1*}, makoto kimura²

¹ 東京大学大学院理学系研究科, ² 茨城大学理学部理学科地球環境科学領域
¹University of Tokyo, ²Ibaraki University

The silicate part of mesosiderites is similar to HED achondrites. The parent body solidified early. Mesosiderites were located close to the surface of the parent body as evidenced by rapid cooling rates after a reheating event (Delaney et al., 1981) and also by excess neutron fluence (Hidaka and Yoneda, 2011). Hence mesosiderites may remember the early solar nebula environment which was very energetic as suggested by chondrule formation. In fact, mesosiderites were reheated to high temperatures after the mixing of silicates and metal. The heat source of this reheating event is not well established and mesosiderites may have been heated by an external (nebular) heat source. For understanding mesosiderite formation and the reheating event we need to study the most primitive mesosiderites. The following features can be used as criteria for primitiveness. They are plagioclase composition heterogeneity, pyroxene lamellae width, metal grain size and olivine corona development. Plagioclase compositions in mesosiderites are in a restricted range (Delaney et al., 1981). The compositional variation was probably inherited from the precursor materials though it may be partly due to evaporative loss of Na at high temperatures. In either case, the heterogeneity would be reduced during subsequent cooling in a closed system. A wider compositional range could be an indicator for weaker reheating. Plagioclase in NWA 1878 shows the widest range in composition, ranging from An79 to An99. This was measured with SEM-EDS and need to be confirmed by EPMA. Pyroxene lamellae width seems to be a promising criterion because this is not affected by original heterogeneity of brecciated samples. But in order to make this a quantitative criterion, bulk pyroxene composition effects have to be corrected because the exsolution temperature depends on the bulk pyroxene composition. In the case of NWA 1878, pyroxene lamellae are observed only in Fe-rich pyroxenes (Fs38-Fs43). This suggests relatively rapid cooling, although the exact cooling rate has not been established yet. The metal grain size seems to be a good criterion for relatively primitive mesosiderites which show spheroidal metal grains. The size determination was made by fitting spheroids to spheroidal grains. This procedure is somewhat subjective because grains are not perfectly spheroidal, somewhat sintered with each other. As the grain size grows by metamorphism, the metal shape becomes more irregular and quantitative size determination becomes more difficult. In spite of such difficulties, metal grain sizes could be determined precise enough for the purpose of sub-classification of primitive mesosiderites. The metal size is ~250 micrometer in diameter in NWA 1878 which is the smallest among the mesosiderites in this study. Incipient corona formation around an olivine grain ~2 micrometer in size is observed in NWA 1878. Fe-poor pyroxenes occur close to the olivine, followed by anorthite. Chromites are located farther away in Fe-rich pyroxenes. Many phosphates are found on metal grains facing the olivine. These are in contrast with stage I corona described by Nehru et al., (1980) and Delaney et al., (1981) where chromites are located in a distinct corona layer next to the olivine and many phosphates are also located close to the corona. The locations of chromite and phosphate in NWA 1878 suggest that both Cr and P did not diffuse over long distances during the reheating event. This petrographic feature cannot be quantized, however, and should be used as supporting evidence for primitiveness. Based on the four criteria, NWA 1878 appears to be the most primitive mesosiderites among 7 mesosiderites I observed so far.

References. Delaney et al., (1981) Proc. Lunar Planet. Sci., 12B, 1315-1342. Hidaka and Yoneda, (2011) GCA 75, 5706-5715. Nehru et al., (1980) GCA 44, 1103-1118.

キーワード: メソシデライト, 再加熱, 始原的
Keywords: mesosiderite, reheating, primitive

NWA801 CR2 コンドライト中のグラファイトを含む岩相と含まない岩相を持つ火成岩的クラストの起源 Origin of igneous clasts with graphite-bearing and graphite-free lithologies found in NWA801 (CR2) chondrite

比屋根 肇^{1*}, 杉浦 直治¹, 木多紀子², 木村 眞³, 三河内 岳¹, 森下 祐一⁴, 竹鼻祥恵¹

Hajime Hiyagon^{1*}, naoji sugiura¹, Noriko T. Kita², Makoto Kimura³, Takashi Mikouchi¹, Yuichi Morishita⁴, Yoshie Takehana¹

¹ 東京大学大学院理学系研究科地球惑星科学専攻, ² ウィスコンシン大学マディソン校地球科学科, ³ 茨城大学理学部, ⁴ 産業技術総合研究所 地質情報研究部門 マグマ熱水鉱床研究グループ

¹Department of Earth & Planetary Science, Graduate School of Science, The University of Tokyo, ²Department of Geoscience, University of Wisconsin-Madison, ³Faculty of Science, Ibaraki University, ⁴Institute of Geology and Geoinformation, Geological Survey of Japan, AIST

Introduction: We found three igneous clasts in a primitive CR2 chondrite, NWA801. The clasts contain eclogitic mineral assemblages (garnet and omphacite), suggesting formation at a high pressure [1]. The origin of the high pressure could be either due to shock loading or static pressure in deep interior of a large planetesimal. We discuss here the origin of the clasts based on mineralogy, bulk chemistry, oxygen isotopes and REE abundances. Preliminary results and arguments are given in [2]. Analytical procedures for oxygen isotopes using a CAMECA ims-1280 ion microprobe at the University of Wisconsin-Madison are given in [3] and those for REE and Ba abundances are briefly described in [2] (also see [4]).

Two lithologies: The igneous clasts have two different lithologies: graphite-bearing (GBL) and graphite-free (GFL). The constituent minerals are olivine, Ca-poor pyroxene, Na-Al-rich pyroxene (omphacite) and garnet, with minor minerals such as graphite (in GBL), phlogopite (in GFL), chlorapatite, Fe-Ni metal, troilite and pentlandite. The mineral assemblages and compositions are similar to those in terrestrial eclogite. The formation condition of the clasts is estimated to be ~3GPa and ~1000C based on a set of conventional geothermobarometers [1].

Bulk chemical compositions of both GBL and GFL are nearly chondritic (not very different from those of CR chondrites). This suggests that the igneous fractionation is not as extensive as that of ureilites.

Phosphate shows very high LREE abundances (140-200 x CI) and gradual decrease from Gd to Lu (down to 30-50 x CI). Garnet shows rapid increase toward HREE with Lu abundance ~100 x CI for GFL garnet (consistent with garnet/melt partition) but only to ~20 x CI for GBL garnet. Omphacite in GFL shows REE abundances of ~1 x CI. The estimated bulk REE abundances for GFL and GBL show almost flat patterns with ~2 x CI and ~1.5 x CI, respectively. This also suggests that the igneous fractionation is not as extensive as that of ureilites.

Oxygen isotopic compositions of olivine and pyroxene are distributed along a slope ~0.6 line with one end near the ureilite field [5] and the other near the CR chondrite field [6]. The GFL data are tightly clustered at the upper-right end of the distribution ($\delta^{18}\text{O}$ ~5 permil and $\delta^{17}\text{O}$ ~0.7 permil), whereas the GBL data are more scattered along the line (with $\delta^{18}\text{O}$ from +2.4 to +4.3 permil and $\delta^{17}\text{O}$ from -1.0 to +0.2 permil). There is no particular difference between olivine and pyroxene data.

Discussion: The formation conditions estimated from several geothermobarometers gave consistent results (~3GPa and ~1000C [1]). This suggests that equilibration has been attained among different mineral assemblages. This favors a static high pressure model. However, the REE and oxygen isotope data show noticeable heterogeneity within and/or between the two lithologies. This seems to support a shock-induced high pressure model, though it is not certain if a shock heating event with a rather short heating duration (~10 sec) could produce all the observed features of the igneous clasts. In any case, rather large planetesimals and their disruptions must be required to produce two different lithologies of the igneous clasts, to stick them together, and mix them with chondrules and matrices to form a CR chondrite.

References: [1] Kimura M. et al. (2013) *Amer. Mineral.*, 98, 387-393. [2] Hiyagon H. et al. (2012) *Antarctic Meteorites XXXV* (abstract), 17-18. [3] Kita N. T. et al. (2009) *Chem. Geol.* 264, 43-57. [4] Hiyagon H. et al. (2012) *Geochim. Cosmochim. Acta* 75, 3358-3384. [5] Kita N. T. et al. (2004) *Geochim. Cosmochim. Acta* 68, 4213-4235. [6] Clayton R. N. and Mayeda T. K. (1999) *Geochim. Cosmochim. Acta* 63, 2089-2104.

Japan Geoscience Union Meeting 2013

(May 19-24 2013 at Makuhari, Chiba, Japan)

©2013. Japan Geoscience Union. All Rights Reserved.



PPS02-13

会場:203

時間:5月20日 14:30-14:45

キーワード: CR コンドライト, 火成岩的クラスト, グラファイト, 酸素同位体, 希土類元素, 二次イオン質量分析
Keywords: CR chondrite, igneous clast, graphite, oxygen isotopes, REE, SIMS

Heterogeneous impact processes and shock scale problem Heterogeneous impact processes and shock scale problem

関根 利守^{1*}

Toshimori Sekine^{1*}

¹ 広島大学 地球惑星システム学専攻

¹DEPSS, Hiroshima University

Shock processes are time-, space-, and initial state-dependent so that they display complicated and non-equilibrium phenomena. In order to understand them from the meteorites that experienced impacts, it is not so simple as we can imagine based on the detailed observations of meteorites. We need to develop more models to help us to know the basis of shock-induced chemical, mineralogical, and physical processes of various states of meteorite materials. Heterogeneous conditions generated by shock wave are to be characterized by the initial state of pre-impact body. Local temperature rise due to local energy deposition makes more difficult to interpret the phenomena. We consider some heterogeneous heating mechanism during shock process.

キーワード: Shock processes, Impact, Experiments, High pressure and high temperature

Keywords: Shock processes, Impact, Experiments, High pressure and high temperature